Food Chemistry: X 15 (2022) 100421

Contents lists available at ScienceDirect

Food Chemistry: X

journal homepage: www.sciencedirect.com/journal/food-chemistry-x

Physicochemical characteristics of *Ganoderma lucidum* oligosaccharide and its regulatory effect on intestinal flora *in vitro* fermentation

Qile Xia [a,1], Qin Zhao [b,c,1], Hua Zhu [b,c], Yan Cao [a], Kai Yang [b,c], Peilong Sun [b,c], Ming Cai [b,c,*]

[a] State Key Laboratory for Managing Biotic and Chemical Threats to the Quality and Safety of Agro-products, Zhejiang Provincial Key Laboratory of Fruit and Vegetables Postharvest and Processing Technology, Ministry of Agriculture and Rural Affairs Key Laboratory of Post-Harvest Handling of Fruits, Institute of Food Science, Zhejiang Academy of Agricultural Sciences, Hangzhou 310021, People's Republic of China

[b] Department of Food Science and Technology, Zhejiang University of Technology, Hangzhou, Zhejiang 310014, People's Republic of China

[c] Key Laboratory of Food Macromolecular Resources Processing Technology Research (Zhejiang University of Technology), China National Light Industry, People's Republic of China

ARTICLE INFO

Keywords:
Ganoderma lucidum oligosaccharide
Structure characteristic
In vitro fermentation
Intestinal flora
Regulatory function

ABSTRACT

This study explored the structure characteristics of an oligosaccharide from *Ganoderma lucidum* (GLO) and its regulatory functions on intestinal flora fermentation *in vitro*. GLO was extracted by ultrasonic-assisted enzymatic hydrolysis, and purified with a dextran gel column. Digestion properties and intestinal flora regulation effects of GLO were investigated by both simulation models. Results showed that GLO was a chain-like homogeneous oligosaccharide, composed of → 6)-β-D-Glcp-(1→, →4)-α-D-Glcp-(1→, β-D-Glcp-(1→, α-D-Manp-(1 →. Its structure could not be easily degraded by digestion in the mouth, gastric and small intestine. Accordingly, they can be utilized by the intestinal flora in large intestine. By evaluating the gas, short chain fatty acids, pH and flora abundance *in vitro* fermentation, it indicated that GLO had good regulatory effects on intestinal flora. Accordingly, GLO might be a potential prebiotic applied in functional foods.

Introduction

Intestinal flora, numerous and diverse, is considered as an invisible organ to human beings (Sedzikowska & Szablewski, 2021). The balance of intestinal flora is very important for human health. By regulating intestinal flora, we can regulate host signal pathway, shape immune system, resist pathogens and prevent microbial overgrowth (Yu, Jobin, & Thomas, 2021). In recent years, dietary intervention became an effective strategy to regulate microbial composition in intestinal tract (Weir, Trikha, & Thompson, 2021). As a unique natural resource, edible and medicinal fungi have been received extensive attention in the fields of health care products and medicines, especially their active ingredients on intestinal flora (Jayachandran, Chen, Chung, & Xu, 2018).

Ganoderma lucidum is a porous fungus, which used in dietary supplements and functional foods with the effects of anti-oxidation, lowering blood pressure, anti-inflammatory and anti-cancer. It contains active components of polysaccharides, nucleosides, triterpenoids, alkaloids, amino acids, proteins and others (Zheng, Zhang, & Liu, 2020). In recent decades, a large number of studies focused on the polysaccharides from *Ganoderma lucidum*, which have good regulatory effects on neurological, immune, cardiovascular and other diseases. However, the functional activity of *Ganoderma lucidum* polysaccharides is still limited due to their low solubility and bioavailability (Zhu, Ni, Xiong, & Yao, 2021). Oligosaccharides, which have small molecular weights and higher solubility, might be an alternative ingredient in *Ganoderma lucidum*, however, studies on their structures and regulatory effects on intestinal flora are limited.

Oligosaccharides are saccharides between monosaccharides and polysaccharides, generally with a low degree of polymerization formed by the condensation of 2–10 monosaccharides. Compared with polysaccharides, oligosaccharides generally have higher solubility and bioavailability. As an important prebiotic, oligosaccharides can treat and alleviate intestinal diseases by regulating intestinal flora. In recent years, a large number of studies have confirmed the prebiotic function of oligosaccharides (Jiang, Cheng, Liu, Sun, & Mao, 2021). Gomez et al. (2014) found that the number of *Bifidobacterium* and *Lactobacillus* in the

* Corresponding author at: Department of Food Science and Technology, Zhejiang University of Technology, Hangzhou, Zhejiang 310014, People's Republic of China.
E-mail address: caiming@zjut.edu.cn (M. Cai).
[1] These authors contributed to the work equally and should be regarded as co-first authors.

https://doi.org/10.1016/j.fochx.2022.100421
Received 1 April 2022; Received in revised form 4 August 2022; Accepted 5 August 2022
Available online 9 August 2022

fermentation broth increased when using the orange peel oligosaccharides as a fermentation substrate. It was also found that oligosaccharides mixture, obtained from the hydrolysis of beet residue and lemon peel residue, could significantly increase the contents of beneficial bacteria such as *Bifidobacterial*, *Lactobacilli*, *Faecalibacterium* and *Roseburia* (Gómez, Gullón, Yáñez, Schols, & Alonso, 2016). In our previous study, we found the prebiotic activity of *Hericium erinaceus* oligosaccharides was significant (Cai, Chen, Ma, Yang, & Sun, 2019). When the oligosaccharides accounts for 25 % of carbon source, the number of *Lactobacillus* increased the fastest.

In this study, *Ganoderma lucidum* oligosaccharide (GLO) was prepared by ultrasound-assisted enzymatic extraction and gel column purification, and its structure was identified. Additionally, characteristics of its digestion and regulation effects on intestinal flora were explored by simulated digestion and fermentation *in vitro*.

Materials and methods

Materials and chemicals

Spray-dried powder of *Ganoderma lucidum* water extracts was supplied by Longevity Valley Botanical Co. ltd. (Jinhua, Zhejiang, China). Cellulase (50 U/mg) purchased from Shanghai Yuanye Bio-Technology Co., ltd (Shanghai, China). Peptone, beef extract, and yeast extract purchased from Beijing Shuangxuan Microbial Culture Medium Products Factory (Beijing, China). All other chemicals used in this study were of analytical grade.

Preparation of GLO

The extracts powder was dissolved at a solid–liquid ratio of 1:10, followed by enzymatic hydrolysis. The optimal enzymatic hydrolysis conditions were enzyme dosage of 1000 U/g substrate, temperature 50 ℃, hydrolysis time 9 h, and pH 5. The solution after enzymatic hydrolysis was treated by ultrasound (FS-1200, Ningbo SCIENT Z Co., ltd., Zhejiang, China) at an intensity of 4.8 W/mL and time of 60 min. Ultrafiltration with Polyethersulfone 3000 Da membrane (RisingSun Membrane Technology Co., ltd., Beijing, China) was carried out at 1 MPa and 600 r/min. Permeate was collected as crude oligosaccharides, and decolorized by macroporous resin (Zhejiang Kal Biotechnology Co., ltd., Hangzhou, China). The yield of GLO obtained by ultrasound-assisted enzymatic hydrolysis was about 1.76 %.

Purification of GLO

25 mg of crude GLO was dissolved in 5 mL pure water, purified by a Sephadex G25 column (Pharmacia, NYT, USA), eluted with deionized water at a rate of 10 mL/3 min and collected 100 tubes. Total sugar in each 100 tubes was measured by phenol sulfuric acid method and drawn as an elution curve, shown in Fig. S1A. Tubes of the highest peak area fraction between 25 and 35 were collected and purification twice, as shown in Fig. S1B. Purification sample were collected for subsequent experiments.

Determination of molecular weight

Molecular weight of the purified GLO was determined by GPC with a HPLC system (LC-10A, Shimadzu, Japan) equipped with a gel column (BRT105-104–102, BoRui Saccharide, China) and a differential detector (RI-10A, Shimadzu, Japan). Samples and standards were prepared to be 5 mg/mL. After centrifugation at 12,000 rpm for 10 min, the supernatant was filtered with a 0.22 μm microporous membrane, and transferred to a 1.8 mL injection vial. Chromatographic method was carried out according to a literature (Wu et al., 2020) with some modifications as mobile phase 0.05 M NaCl solution, flow rate 0.6 mL/min, column temperature 40 ℃, and injection volume 20 μL.

Analysis of monosaccharide composition

Monosaccharide composition of GLO was analyzed according to Yan's method (Yan et al., 2016). 2 mg/mL different standards of monosaccharide were prepared. Mixed standard was prepared by 100 μL of each standard together. 2 mg of pure oligosaccharide was added with 4 mL of 2 mol/L Trifluoroacetic acid (TFA) and filled with nitrogen, sealed it in an oven at 110 ℃ for 4 h. After cooled to room temperature, it was neutralized with 1 mol/L NaOH to be pH 7.0, and diluted to be 4 mL for later use. The sample was evaporated to be dryness by adding 1 mL of methanol, 5 times repeatedly. After the TFA was completely removed, it was diluted with distilled water to be 2 mL. 400 μL of 0.3 mol/L NaOH and 400 μL of PMP methanol were added to 400 μL of single standard, uniformly mixed in water bath at 70 °C for 1 h, respectively. 0.3 mol/L HCl was added to neutralize all the samples, and 1 mL chloroform was further added. Samples were swirled for 2 min with a vortex oscillator, then discarded the lower organic phase after stood for 5 min. The derivative solution was obtained by filtering the supernatant with a 0.45 μm aqueous membrane. HPLC was carried with a C18 column, mobile phase of phosphoric acid buffer: acetonitrile = 82:18, flow rate 1 mL/min, column temperature 30 °C, UV 245 nm, and injection volume 20 μL.

Nuclear magnetic resonance (NMR) spectroscopy

30 mg of purified GLO was fully dissolved with 0.50 mL of D_2O, carefully loaded it into the nuclear magnetic tube with a syringe. It was determined with a 400 MHz NMR instrument (Bruker 400 M, Germany). ^{1}H NMR, ^{13}C NMR, DEPT-135, ^{1}H–^{1}H COSY, TOCSY, HMQC, HMBC and NOESY spectra were measured.

Simulated digestion

Oral digestion

Oral digestion was carried out according to the method described by Su et al. (2019). Saliva was collected in the morning before eating, provided by three volunteers ranged in ages from 20 to 25 years old and had not received antibiotics for at least three months. Saliva was centrifuged at 4500 r/min for 10 min, and the supernatant was taken for use. 3 groups were prepared, such as 4 mL of GLO solution (8 mg/mL) and 4 mL of saliva, 4 mL of deionized water and 4 mL of saliva, and 4 mL of GLO solution and 4 mL of deionized water. These groups were put into a 40 ℃ water bath for oral digestion simulation. 1 mL of the mixture was collected at 0, 5 and 20 min, respectively, and placed in a boiling water bath for inactivation for 5 min, centrifuged at 4500 r/min for 10 min. The supernatant was collected for determination of the total sugar retention rate (TSR), reducing sugar retention rate (RSR), chemical bond and sugar content as the following equations.

$$TSR(\%) = \frac{TSI}{TSUI} \times 100\%$$

$$RSR(\%) = \frac{RSI}{RSUI} \times 100\%$$

where TSI: total sugar content in digestive juice, TSUI: total sugar content in undigested juice, RSI: reducing sugar content in digestive juice, RSUI: reducing sugar content in undigested liquid.

Gastric digestion

Gastric digestion was carried out according to the method described by Huang et al. (2019). 0.22 g KCl, 0.62 g NaCl, 0.12 g $NaHCO_3$ and 0.05 g $CaCl_2$ were dissolved in 200 mL deionized water, adjusted the pH to be 2.0 with 0.1 mol/L HCl. 35.4 mg pepsin, 37.5 mg gastric lipase and 1 mL CH_3COONa (pH 5.0, 1 mol/L) were added to 150 mL gastric juice medium, and adjusted the pH to be 3.0. Three groups of samples as the same prepared in 2.7.1 were used. The pH of each group was adjusted to

be 3.0 and placed in a 37 °C water bath to simulate gastric juice digestion. During digestion, 1 mL of the mixture was collected for further determination at 0, 2 and 4 h, respectively.

Small intestinal digestion

Small intestinal was carried out according to the method described by Su et al. (2019). 0.065 g KCl, 0.033 g $CaCl_2$ and 0.54 g NaCl were dissolved in 100 mL deionized water, and adjusted the pH to be 7.5 with 0.1 mol/L NaOH. 200 g bile salt solution (4 %, w/w), 6.5 g trypsin, and 50 g pancreatin solution (4 %, w/w) were dissolved in 50 g of small intestinal fluid medium, and adjusted the pH to be 7.5. Three groups were prepared as 30 mL of digested simulated gastric juice and 9 mL of small intestinal juice, 30 mL of deionized water and 9 mL of small intestinal juice, 30 mL of simulated digested gastric juice and 9 mL of deionized water. pH of each group was adjusted to be 7.5 and placed in a 37 ℃ water bath for digestion. 1 mL of the mixture was collected out at 0, 2 and 4 h for further determination, respectively.

Intestinal fermentation in vitro

Preparation of solutions and culture medium

Intestinal fermentation was carried out according to reported methods with slight modifications (Wang et al., 2019). Vitamin I solution: 2 mg cobalamin (VB12), 2 mg biotin (VH), 10 mg folic acid, 6 mg p-aminobenzenesulfonic acid, 30 mg pyridoxamine (VB6) were dissolved in deionized water, and 40 mL of this solution was stored at −30 °C for further use. Metaphosphoric acid solution: 2.5 g of metaphosphoric acid was dissolved in deionized water to be 100 mL with a mass-to-volume ratio of 2.5 %. Crotonic acid-metaphosphoric acid solution: 0.6464 g crotonic acid was fully dissolved in 100 mL of metaphosphoric acid solution. YCFA basic medium: 0.45 g KH_2PO_4, 0.45 g K_2HPO_4, 0.05 g NaCl, 0.064 g $CaCl_2{\cdot}2H_2O$, 0.09 g $MgSO_4{\cdot}7H_2O$, 2.5 g yeast extract, 10 g tryptone, 2 mL heme, 1 g L-cysteine, 200 μL vitamin I, all were dissolved in deionized water to be 1 L. Experimental grouping: 0 g GLO added to 100 mL YCFA basic medium as blank group (K), and 0.8 g GLO added to 100 mL YCFA basic medium as GLO group. Peristaltic pump was used to fill the culture medium into the vials respectively under the condition of nitrogen, with 5 mL for each filling. All the groups were autoclave sterilization.

Preparation of human fecal fluid

5 males and 5 females volunteers, aged 20–25 years old, have not taken antibiotics within 3 months. All volunteers obtained informed and written consent, and this study was approved by the Ethics Committee of Zhejiang Academy of Agricultural Sciences. 0.8 g of feces were placed in an automatic feces machine (Halo Biotechnology Co. ltd., Jiangsu, China) with 8 mL of PBS buffer, and vortexed evenly for later use. 500 μL of fecal diluent were added to the experimental groups, and cultured in an anaerobic incubator at 37 °C.1 mL sample was collected at 0 and 24 h for relevant analysis, respectively.

Determination of fecal fermentation gas composition

The fermentation medium was collected after culturing for 24 h, and the contents of CO_2, H_2, NH_3 and H_2S in the fermentation flask were detected with a gas detector (Hangzhou Hailu Medical Technology Co., ltd., China).

Determination of short-chain fatty acids (SCFAs)

The fermentation medium was collected after culturing for 24 h, concentrations of SCFAs were analyzed according to a reported method (Mao, Huo, & Zhu, 2013). 0.5 mL of the fermentation broth was added with 1 mL of crotonic acid-metaphosphoric acid solution, vortexed for 2 min, and placed in a −30 °C refrigerator for 24 h. After reaction, it was centrifuged at 10,000 r/min at 4 °C for 5 min, and the supernatant was filtered by an aqueous filter. The fermentation broth was measured by a gas chromatography (GC-2010 Plus, Shimadzu, Japan) equipped with a DB-FFAP column (0.32 mm × 30 m × 0.5 μm) with crotonic acid as an internal standard. Injection port parameters: temperature 250 °C, carrier gas N_2, injection volume 1 μL, purge flow 3.0 mL/L, injection mode as split mode (split ratio 5:1), pressure 41.1 kPa, control mode as line speed of 58 cm/*sec*, total flow 12.1 mL/min, column flow 2.3 mL/min. Oven parameters: initial temperature 75 °C, heating rate (rising to 180 °C at 20 °C/min and holding for 1 min, then rising to 220 °C at 40 °C/min and holding for 1 min, the entire program time 8.05 min). FID detector parameters: temperature 250 °C, makeup gas N_2, makeup gas flow 30 mL/min, H_2 flow 40 mL/min, and air flow 400 mL/min.

Determination of pH

Before and after fermentation, 1 mL of the fermentation broth was collected to measure the pH value with a pH meter (PHS-3C, Hangzhou Aolilong Instrument Co., ltd., China).

Determination of bacterial abundance

The fermentation medium was collected after culturing for 24 h, bacterial abundance was determined according to a described method (Wu et al., 2021). Fermentation broth was centrifuged to collect the pellet, and DNA of the sample was extracted with a DNA kit. The extracted genomic DNA was detected by 1 % agarose gel electrophoresis, followed by PCR amplification. According to the designated sequencing region, specific primers with barcode were synthesized. Each sample was replicated 3 times, and PCR products from the same sample were mixed and detected by 2 % agarose gel electrophoresis. PCR products were recovered by cutting gel with AxyPrep DNA gel recovery kit, eluted with Tris-HCl and detected by 2 % agarose electrophoresis. According to the preliminary quantitative results of electrophoresis, the PCR products were detected and quantified by QuantiFluor™-ST blue fluorescence quantitative system, and mixed according to the sequencing amount of each sample. Illumina PE library construction and Illumina PE sequencing were performed, and corresponding biological analysis was performed.

Statistical analysis

All data were expressed as the mean ± standard deviation. SPSS16.0 software (SPSS Inc., Chicago, IL, USA) was used for one-way ANOVA. The significant difference between the two groups was determined by student-Newman-Keuls test. $P < 0.05$ was considered as statistically significant. Origin 2018 software (OriginLab, USA) was used for mapping.

Results and discussion

Physicochemical characteristics of GLO

Molecular weight of GLO

Standard equation of molecular weight was obtained as $y = -2.6836x + 40.199$, $R^2 = 0.9869$. Accordingly, molecular weight of GLO was about 1280 Da, as shown in Fig. S2, which was consistent with the reported study that oligosaccharides isolated from *Ganoderma lucidum* were between 1 and 5 kDa (Tsai et al., 2012).

Monosaccharide compositions of GLO

In Fig. 1A, it showed each monosaccharide standard in a chromatography. Accordingly, compared with the sample chromatography in Fig. 1B, it indicated that GLO was mainly composed of Glc and Man, in which the relative contents were 82.6 % and 15.3 %, respectively.

Structure of GLO

Commonly, the anomeric hydrogen signals of sugar residues are usually located at 4.5–5.5 ppm in ^1H NMR spectrum. Among them, chemical shift of the α-type signal is usually greater than 5.0 ppm, and chemical shift of the β-type signal is usually<5.0 ppm. The signal located

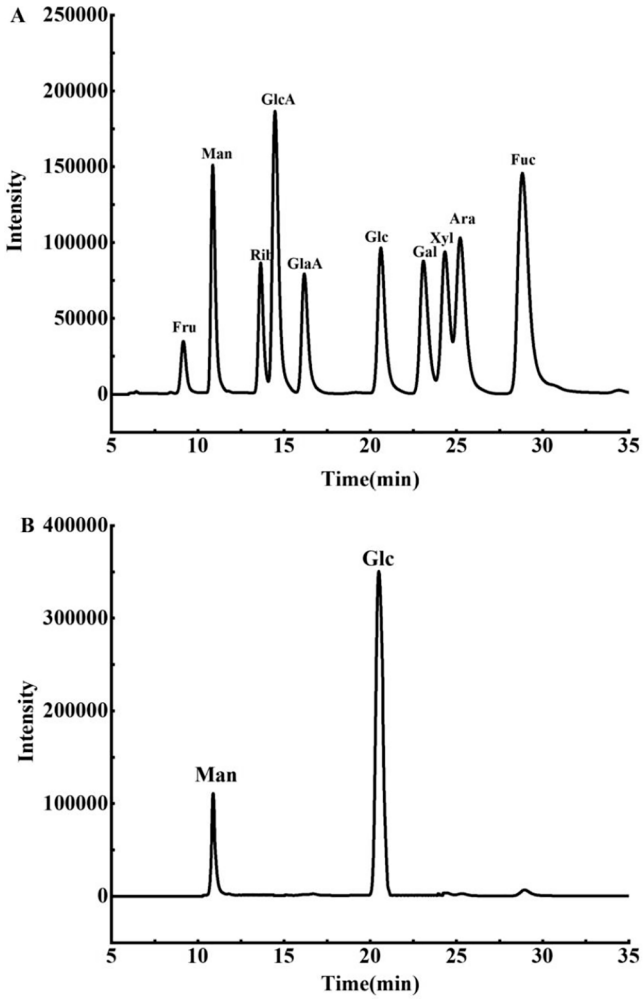

Fig. 1. Chromatography of monosaccharides. A: mixed standard; B: GLO.

at 3.0–4.5 ppm is the hydrogen signal on the oxygen carbon attached to the sugar ring. The hydrogen signals in range of 1.0–2.5 ppm are the methyl hydrogen signals on the sugar ring or the hydrogen signals of the acylated substituents. ^{1}H NMR spectrum of GLO, in Fig. S3A, indicated that there were four groups of hydrogen signals in the anomeric hydrogen signal region, located at 5.36, 5.19, 4.93, and 4.61 ppm, respectively. It was suggested that there were at least 4 different types of sugar residues in this compound, and both α- and β-glycosidic bonds were existed. Other hydrogen signals were in the range of 3.2–4.0 ppm, suggesting that the structure of GLO did not contain monosaccharide types with methyl groups such as Rhamnose and Fucose, nor did it contain other acylated substituents (Ali et al., 2011; Wang et al., 2019). This speculation was consistent with the results of monosaccharide composition.

In Fig. S3B, eight groups of carbon signals could be seen in the anomeric carbon region. Based on the results of monosaccharide composition and molecular weight, it could be speculated that GLO was composed of 8 sugar residues. In Fig. S3C, it indicated that there were positive phase signals in the range of 60–69 ppm, suggesting that the chemical shifts of other oxymethine carbons in GLO were all within this range. The signals in the range of 60–67 ppm were all negative phase, which were attributed to the oxymethylene carbon at the 6-position of the pyranose ring (Wu et al., 2019).

In Fig. S4A, it demonstrated that there were 4 groups of signals in the anomeric hydrogen/carbon region, which were attributed to 4 different sugar residues, suggesting that GLO was composed of 4 different sugar residues. The terminal hydrogen/carbon signal at 4.93/97.8 ppm was the main sugar residue signal, which could be assigned to the 1-position hydrogen/carbon signal of β-D-Glcp, according to the results of monosaccharide composition and chemical shift. In Fig. S4B, the hydrogen signal at 4.93 ppm was correlated with the hydrogen signals at 3.44, 3.53, 3.69, 3.88, 3.73, 3.93. Therefore, the above signals could be assigned to the same spin-coupling system, which was the hydrogen signal on the same sugar ring. In Fig. S4C, there were cross-peak signals located at δH/H 4.93/3.53, 3.53/3.69, 3.69/3.88, 3.88/3.44, 3.44/3.73, 3.73/3.93, suggesting that hydrogen in sugar residues of attribution. According to information in Figs. S4A and S4D, carbon signals of the sugar residue were assigned in Table S1. For convenience of representation, this sugar residue was labeled as Residue A. According to the results of monosaccharide composition and chemical shift, they were assigned to sugar residues with different connection methods. Their types belonged to α-D-Glcp, β-D-Glcp, and α-D-Manp (Zeng et al., 2020; Zhang, Guo, Yan, Feng, & Wan, 2020), marked as Residue B, D, and E, respectively. According to the number of carbon signals and integrated area analysis of the hydrogen spectrum signals, molar ratio of the four sugar residues was 4: 2: 1: 1.

The linking sites and sequences between sugar residues were analyzed by HMBC spectrum and NOESY spectrum, as in Figs. S4D and S4E, respectively. In Fig. S4D, H-6 (3.73/3.93 ppm) of Residue A had a correlation signal with C-1 (97.8 ppm) of Residue A, suggesting that C-6 of Residue A was connected to O-1 of Residue A. Similarly, there were related peaks at 3.93/99.8 ppm (AH6/BC1), 3.93/95.9 ppm (AH6/DC1), 5.19/97.8 ppm (EH1/AC1), indicating that C-6 of Residue A was linked to O-1 of Residue B, C-6 of Residue A was connected to O-1 of Residue D, C-1 of Residue E was connected to O-1 of Residue A. In addition, the crossing peaks of H-1(4.93 ppm) of Residue A and H-4(3.59 ppm) of Residue B existed in the NOESY spectra, suggesting that C-4 of Residue B was connected with O-1 of Residue A. The results indicated that GLO could be a chain oligosaccharide composed of → 6)-β-D-Glcp-(1→, →4)-α-D-Glcp-(1→, β-D-Glcp-(1→, α-D-Manp-(1→ (Ali et al., 2011; Wang et al., 2019).

According to all the results of monosaccharide composition, molecular weight and NMR, GLO in current study was a chain-like homogeneous oligosaccharide, composed of → 6)-β-D-Glcp-(1→, →4)-α-D-Glcp-(1→, β-D-Glcp-(1→, α-D-Manp-(1→, as proposed in Fig. 2.

Characteristics changes of GLO in digestion and fermentation

Changes in retention of TSR

During digestion, oligosaccharides could change in chemical composition, sugar content, characteristic bonds, and these might lead to alter their biological activities. When humans ate foods, it first stayed in mouth for 10 s − 2 min, and accordingly stayed in the gastric for 15 min-3 h, in the small intestine for 2–5h, and finally in the large intestine for 12–24 h (Min, Hu, Nie, Xie, & Xie, 2014). In Fig. 3, it indicated GLO had no significant changes in TSR and RSC after being digested by simulated oral fluid, gastric fluid and small intestinal fluid. But after 24 h fermentation in large intestine, TSR of GLO was significantly decreased ($p < 0.05$). The rates of TSR and RSR were 63.26 % and 41.33 %, respectively, similar to the results reported in literature (Chen et al., 2018). Result showed that GLO could not easily be decomposed in mouth, gastric and small intestine, and smoothly entered into the large intestine. Accordingly, GLO might be utilized by intestinal microbes and became carbon sources for microbial growth and utilization.

Changes in content

In Fig. S5, it indicated that the main characteristic peaks of GLO did not change significantly after being digested by oral fluid, gastric fluid and small intestinal fluid. Contrarily, the peak area of GLO was significantly reduced after being fermented in large intestine. It demonstrated that GLO would be degraded and utilized by microorganisms in large intestine.

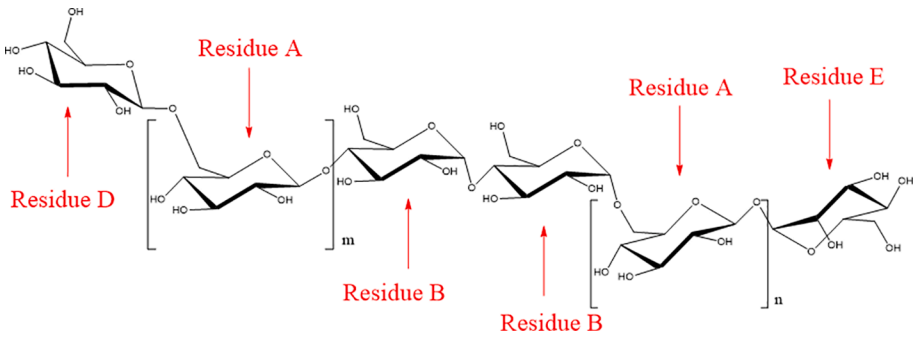

Fig. 2. Proposed structural of GLO (m + n = 4).

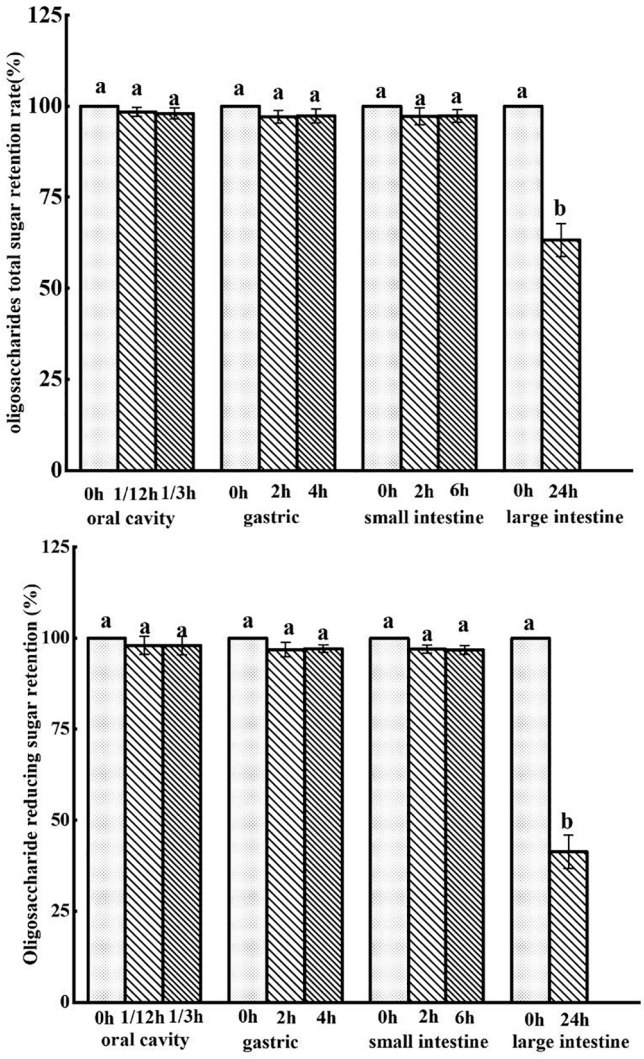

Fig. 3. Total sugar retention and reducing sugar retention of GLO in simulated digestion.

Changes in structural characteristics

As shown in Fig. S6, GLO had O—H stretching vibration absorption peaks in the range of 3257.9 cm^{-1}-3261.9 cm^{-1}, and stretching vibration absorption peaks of C—H (2919.6 cm^{-1}-2927.5 cm^{-1}), C—C (1587.9 cm^{-1}-1597.6 cm^{-1}), C—H (1412.9 cm^{-1}-1414.7 cm^{-1}). An absorption peak appeared in the range of 1138.9 cm^{-1}-1148.9 cm^{-1}, indicating that the existence of pyranose (Zhang et al., 2020). As a result, FTIR spectra of GLO did not change after digestion in all stages, indicating that the structure of GLO was stable during the process.

Effects of GLO on intestinal microflora in vitro fermentation

Gas components

Changes of chemicals and microbial flora in intestinal tract can cause changes of gas, such as CO_2, H_2, NH_4 and H_2S, which lead to affect human health (Ou et al., 2015). In Fig. 4A, the content of total gases in GLO group increased compared with the blank. H_2 in the gut mainly comes from bacterial fermentation, and carbohydrate intake can increase its content (Kalantar-Zadeh, Berean, Burgell, Muir, & Gibson, 2019). Hydrogen-producing microorganisms, such as *Roseburia*, *Clostridium* and *Bacteroides*, can also convert H_2 into CH_4 and H_2S. As shown in Fig. 4B, the content of H_2 in GLO group increased significantly ($p < 0.05$), indicating that GLO could promote the growth of intestinal hydrogen-producing bacteria.

As a common intestinal gas, H_2S can induce some intestinal diseases at low doses, such as colitis (Szilagyi et al., 2007). When the content of H_2S is high, it is harmful for the human body. For example, the coexistence of H_2S and NO would weak β-oxidation and protein synthesis. The production of H_2S was mainly associated with sulfate-reducing bacteria and protein-fermenting bacteria (Yao, Muir, & Gibson, 2016). As shown in Fig. 4C, H2S content in the GLO group decreased significantly ($p < 0.05$), indicating that GLO might inhibit the growth of H_2S-producing bacteria.

As an inert gas, CO_2 only produces mechanical stimulation to the body in the intestinal tract (Yao et al., 2016). CO_2 is also closely related to the production of CH_4, and methanogens can convert CO_2 and H_2 into CH_4. In Fig. 4D, CO_2 production in the GLO group was higher than that in the blank ($p < 0.05$).

NH_3 is generally formed by the decomposition of undigested protein and its hydrolyzed amino acids by intestinal bacteria. The presence of high content of NH_3 could trigger some intestinal diseases (Kurada, Alkhouri, Fiocchi, Dweik, & Rieder, 2015). In Fig. 4E, NH_3 in GLO group decreased ($p < 0.05$) which demonstrated GLO could inhibit the growth of NH_3-producing microorganisms.

Short-chain fatty acid (SCFA)

SCFA, including acetic acid, propionic acid, butyric acid, isobutyric acid, valeric acid, isovaleric acid and other trace acids, are produced by the fermentation of carbohydrates with gut anaerobic microorganisms which have an important relationships with human health (van der Hee and Wells, 2021). *Bifidobacterium*, *Lactobacillus*, *Akkermansia* and *Provostella* are the main acetic acid-producing microorganisms, which can regulate the pH value in the intestinal tract and control human appetite by producing acetic acid. It can nourish butyrate-producing microorganisms, thereby preventing intestinal diseases. *Bacteroidetes* are the main propionic acid-producing bacteria, which can play anti-inflammatory and anti-cancer functions by producing propionic acid. *Faecalibacterium prausnitzii* and *Roseburia* are butyric acid-producing bacteria that can help prevent intestinal gas leaks and fight inflammation and cancer (Fernández et al., 2016). In Fig. 5A, after 24 h fermentation, the total acid content in GLO group was significantly higher than

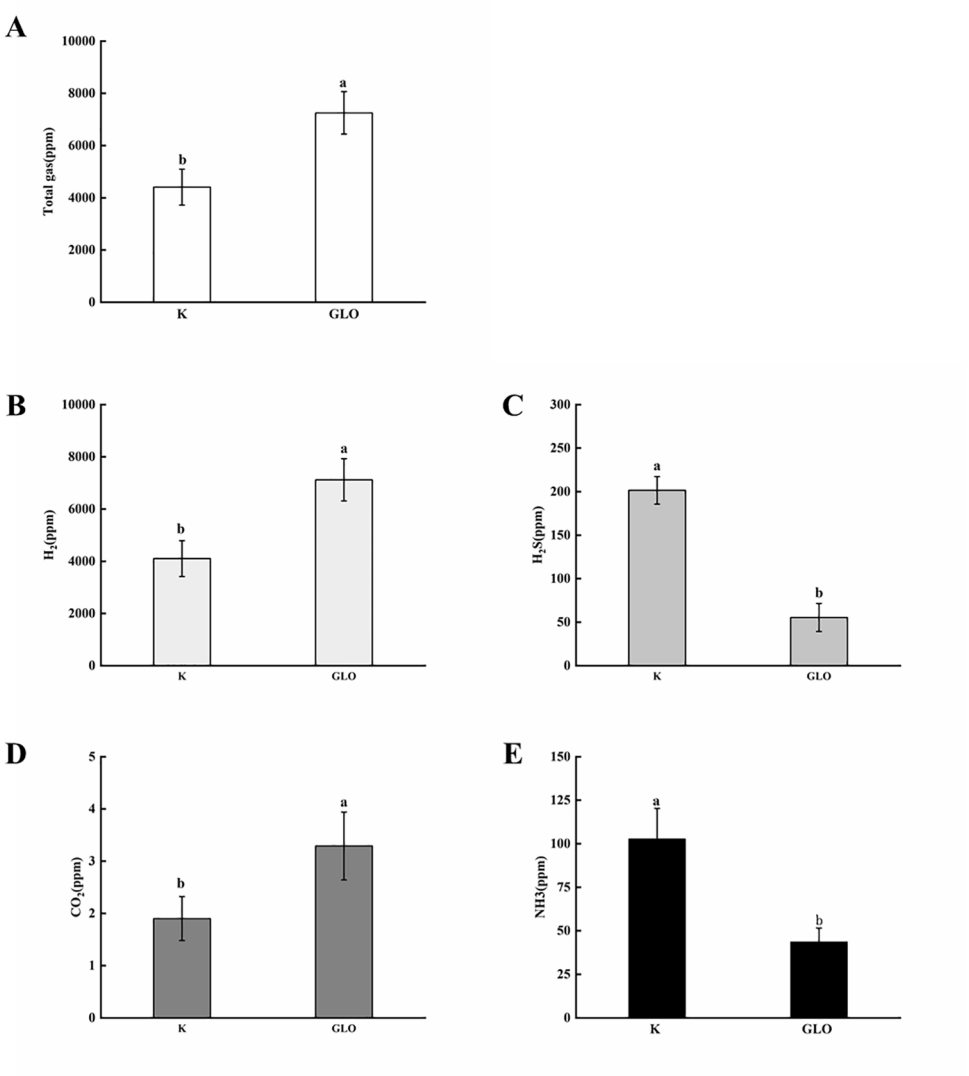

Fig. 4. Gas changes before/after fermentation *in vitro*. K: Blank group; GLO: GLO group. A: Total gas; B: H_2; C: H_2S; D: CO_2; E: NH_3.

that in the blank ($p < 0.05$). In Fig. 5B-5G, it showed all the acids in the GLO group became higher, indicating GLO had positive effects on gut microorganisms.

pH

SCFAs can inhibit the growth of intestinal pathogens and reduce the probability of colon cancer by regulating intestinal pH (Tan et al., 2014), which can be used as an index by the utilization of carbohydrates. In Fig. S7, it showed that after 24 h fermentation, pH of the GLO group decreased significantly ($p < 0.05$), however, it increased in the blank group. Accordingly, GLO have a better effect on the proliferation of acid-producing microorganisms.

Intestinal flora abundance

Human health has an important relationship with the structure of gut microbiota (Cunningham et al., 2021). Some intestinal diseases can be prevented and improved by exploring the relationship between dietary regulation and intestinal flora.

At the phylum level, intestinal flora is mainly divided into Firmicutes, Bacteroidota, Proteobacteria and Actinobacteria. Several studies have found that Firmicutes could degrade glycans, thereby increasing their utilization (Ndeh & Gilbert, 2018). As shown in Fig. 6A, the relative abundance of Firmicutes in GLO group increased. The relative abundance of Bacteroidota in GLO medium increased significantly ($p < 0.05$), which verified that GLO was degraded and utilized. Proteobacteria are intestinal pathogens that can make human diseases (Shin, Whon, & Bae, 2015). The relative abundance of Proteobacteria in GLO group was significantly decreased ($p < 0.05$). Actinobacteria, increased in GLO group, is one of the four major bacterial phyla in the body, which can degrade complex polymers.

At the genus level, *Lactobacillus* and *Bifidobacterium* are typical intestinal beneficial bacteria. It can inhibit the growth of harmful intestinal bacteria by fermenting sugar substances to produce lactic acid, butyric acid, etc., reducing the production of toxins (Yang, Martinez, Walter, Keshavarzian, & Rose, 2013). *Faecalibacterium*, beneficial intestinal bacteria, can produce butyrate and CO_2 in the colon, and has anti-obesity and anti-inflammatory effects (La Fata et al., 2017). Some studies found that *Prevotella* in the human gut has a regulatory effect on gut health, and it can improve glycogen storage capacity by improving glucose metabolism (Kovatcheva-Datchary et al., 2015). *Escherichia-Shigella* are usually harmful bacteria in the gut, and their overgrowth can produce Shiga toxin, causing symptoms such as diarrhea (Khan & Chousalkar, 2020). As shown in Fig. 6B, the relative abundance of beneficial bacteria such as *Lactobacillus*, *Bifidobacterium*, *Faecalibacterium*, and *Prevotella* in the GLO group increased significantly ($p < 0.05$). The relative abundance of some harmful bacteria such as *Escherichia-Shigella* and *Dorea* decreased significantly ($p < 0.05$). GLO could modulate gut health by increasing the relative abundance of beneficial

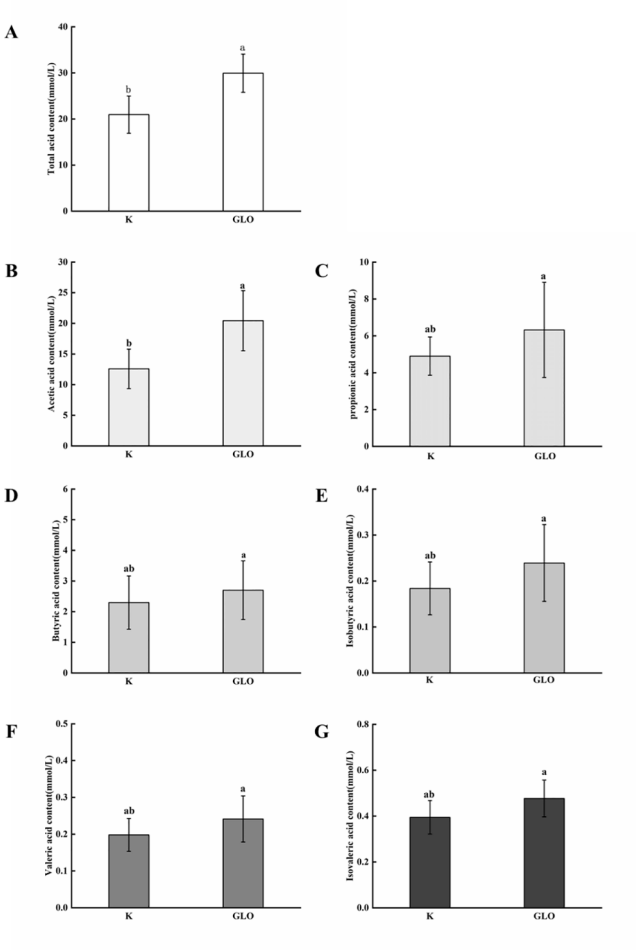

Fig. 5. SCFAs changes before/after fermentation *in vitro*. K: Blank group; GLO: GLO group. A: total acid; B: acetic acid; C: propionic acid; D: butyric acid; E: isobutyric acid; F: valeric acid; G: isovaleric acid.

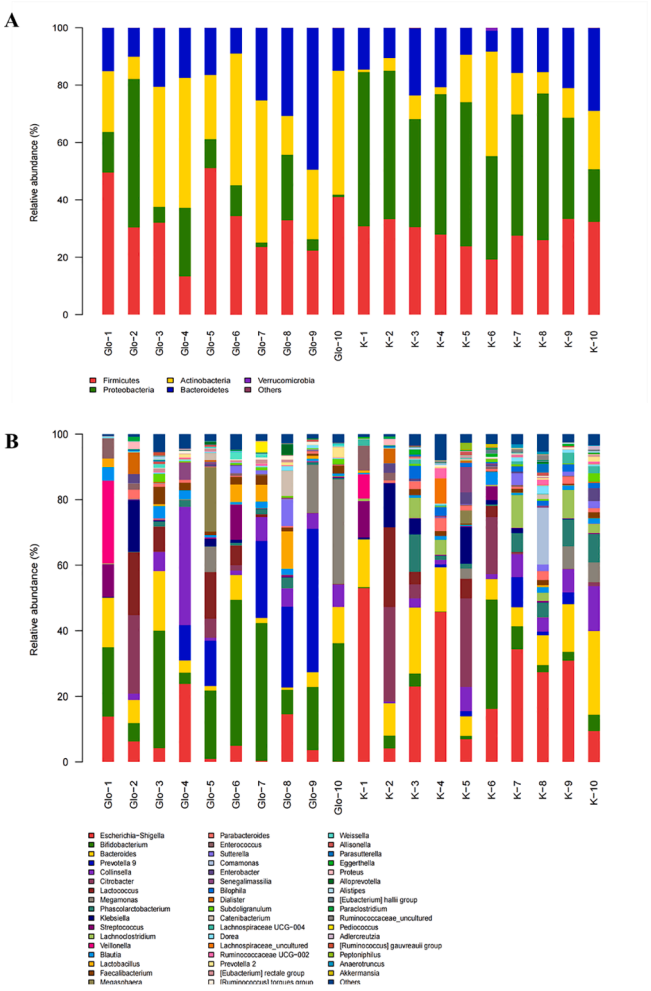

Fig. 6. Relative abundance of intestinal flora in GLO and blank groups at phylum level (A) and genus level (B). K: Blank group; GLO: GLO group. Note: GLO/K-12345678910 refers to 10 different feces.

gut bacteria and reducing the harmful gut bacteria.

Conclusions

In this study, an oligosaccharide of *Ganoderma lucidum* with a molecular weight of about 1280 Da was obtained by ultrasonic-assisted enzymatic hydrolysis and dextran gel column. GLO mainly composed of Glucose and Mannose, with the relative contents of 82.6 % and 15.3 %, respectively. According to the results of NMR, it proved that GLO was a chain-like homogeneous oligosaccharide composed of → 6)-β-D-Glcp-(1→, →4)-α-D-Glcp-(1→, β-D-Glcp-(1→, α-D-Manp-(1→.

GLO remained unchanged during the simulated digestions in the oral cavity, gastric and small intestine. After colonic fermentation *in vitro*, the retention rate of total sugar, total reducing sugar, and the sugar content decreased significantly, but the characteristic bonds remained unchanged. GLO had good regulation effects on intestinal flora according to the results of gas, SCFAs, pH and bacterial structure in the simulated fermentation. The relative abundance of beneficial bacteria such as *Lactobacillus*, *Bifidobacterium*, *Faecalibacterium*, and *Prevotella* increased significantly by treatment of GLO, while some harmful bacteria such as *Escherichia-Shigella* and *Dorea* decreased significantly. GLO could modulate gut health by increasing the relative abundance of beneficial gut bacteria and reducing the harmful gut bacteria. The structure–activity relationship will be investigated in our further studies. Oligosaccharide from *Ganoderma lucidum* is a potential resource for functional food.

CRediT authorship contribution statement

Qile Xia: Formal analysis, Data curation, Validation. **Qin Zhao:** Methodology, Investigation, Writing – original draft. **Hua Zhu:** Validation. **Yan Cao:** Formal analysis. **Kai Yang:** Resources. **Peilong Sun:** Supervision. **Ming Cai:** Project administration, Conceptualization, Writing – review & editing.

Declaration of Competing Interest

The authors declare that they have no known competing financial interests or personal relationships that could have appeared to influence the work reported in this paper.

Acknowledgment

This work was supported financially by the Key Research and Development Projects of Zhejiang (2019C02100, 2019C02040).

Appendix A. Supplementary data

Supplementary data to this article can be found online at https://doi.org/10.1016/j.fochx.2022.100421.

References

Ali, I. A. I., Akakabe, Y., Moonmangmee, S., Deeraksa, A., Matsutani, M., Yakushi, T., & Matsushita, K. (2011). Structural characterization of pellicle polysaccharides of Acetobacter tropicalis SKU1100 wild type and mutant strains. *Carbohydrate Polymers, 86*(2), 1000–1006.

Cai, M., Chen, S., Ma, Q., Yang, K., & Sun, P. (2019). Isolation of crude oligosaccharides from Hericium erinaceus by integrated membrane technology and its proliferative activity. *Food Hydrocolloids, 95*, 426–431.

Chen, G., Xie, M., Wan, P., Chen, D., Ye, H., Chen, L., & Liu, Z. (2018). Digestion under saliva, simulated gastric and small intestinal conditions and fermentation in vitro by human intestinal microbiota of polysaccharides from Fuzhuan brick tea. *Food Chemistry, 244*, 331–339.

Cunningham, M., Azcarate-Peril, M. A., Barnard, A., Benoit, V., Grimaldi, R., Guyonnet, D., & Gibson, G. R. (2021). Shaping the Future of Probiotics and Prebiotics. *Trends in Microbiology, 29*(8), 667–685.

Fernández, J., Redondo-Blanco, S., Gutiérrez-del-Río, I., Miguélez, E. M., Villar, C. J., & Lombó, F. (2016). Colon microbiota fermentation of dietary prebiotics towards short-chain fatty acids and their roles as anti-inflammatory and antitumour agents: A review. *Journal of Functional Foods, 25*, 511–522.

Gomez, B., Gullon, B., Remoroza, C., Schols, H. A., Parajo, J. C., & Alonso, J. L. (2014). Purification, characterization, and prebiotic properties of pectic oligosaccharides from orange peel wastes. *Journal of Agricultural and Food Chemistry, 62*(40), 9769–9782.

Gómez, B., Gullón, B., Yáñez, R., Schols, H., & Alonso, J. L. (2016). Prebiotic potential of pectins and pectic oligosaccharides derived from lemon peel wastes and sugar beet pulp: A comparative evaluation. *Journal of Functional Foods, 20*, 108–121.

Huang, F., Liu, Y., Zhang, R., Bai, Y., Dong, L., Liu, L., & Zhang, M. (2019). Structural characterization and in vitro gastrointestinal digestion and fermentation of litchi polysaccharide. *International Journal of Biological Macromolecules, 140*, 965–972.

Jayachandran, M., Chen, J., Chung, S. S. M., & Xu, B. (2018). A critical review on the impacts of beta-glucans on gut microbiota and human health. *Journal of Nutritional Biochemistry, 61*, 101–110.

Jiang, C., Cheng, D., Liu, Z., Sun, J., & Mao, X. (2021). Advances in agaro-oligosaccharides preparation and bioactivities for revealing the structure-function relationship. *Food Research International, 145*, Article 110408.

Kalantar-Zadeh, K., Berean, K. J., Burgell, R. E., Muir, J. G., & Gibson, P. R. (2019). Intestinal gases: Influence on gut disorders and the role of dietary manipulations. *Nature Reviews Gastroenterology & Hepatology, 16*(12), 733–747.

Khan, S., & Chousalkar, K. K. (2020). Salmonella Typhimurium infection disrupts but continuous feeding of Bacillus based probiotic restores gut microbiota in infected hens. *Journal of Animal Science and Biotechnology, 11*, 29.

Kovatcheva-Datchary, P., Nilsson, A., Akrami, R., Lee, Y. S., De Vadder, F., Arora, T., & Backhed, F. (2015). Dietary Fiber-Induced Improvement in Glucose Metabolism Is Associated with Increased Abundance of Prevotella. *Cell Metabolism, 22*(6), 971–982.

Kurada, S., Alkhouri, N., Fiocchi, C., Dweik, R., & Rieder, F. (2015). Review article: Breath analysis in inflammatory bowel diseases. *Alimentary Pharmacology and Therapeutics, 41*(4), 329–341.

La Fata, G., Rastall, R. A., Lacroix, C., Harmsen, H. J. M., Mohajeri, M. H., Weber, P., & Steinert, R. E. (2017). Recent Development of Prebiotic Research-Statement from an Expert Workshop. *Nutrients, 9*(12).

Mao, S., Huo, W., & Zhu, W. (2013). Use of pyrosequencing to characterize the microbiota in the ileum of goats fed with increasing proportion of dietary grain. *Current Microbiology, 67*(3), 341–350.

Min, F. F., Hu, J. L., Nie, S. P., Xie, J. H., & Xie, M. Y. (2014). In vitro fermentation of the polysaccharides from Cyclocarya paliurus leaves by human fecal inoculums. *Carbohydrate Polymers, 112*, 563–568.

Ndeh, D., & Gilbert, H. J. (2018). Biochemistry of complex glycan depolymerisation by the human gut microbiota. *FEMS Microbiology Reviews, 42*(2), 146–164.

Ou, J. Z., Yao, C. K., Rotbart, A., Muir, J. G., Gibson, P. R., & Kalantar-zadeh, K. (2015). Human intestinal gas measurement systems: In vitro fermentation and gas capsules. *Trends in Biotechnology, 33*(4), 208–213.

Sedzikowska, A., & Szablewski, L. (2021). Human Gut Microbiota in Health and Selected Cancers. *International Journal of Molecular Sciences, 22*(24).

Shin, N. R., Whon, T. W., & Bae, J. W. (2015). Proteobacteria: Microbial signature of dysbiosis in gut microbiota. *Trends in Biotechnology, 33*(9), 496–503.

Su, A., Ma, G., Xie, M., Ji, Y., Li, X., Zhao, L., & Hu, Q. (2019). Characteristic of polysaccharides from Flammulina velutipes in vitro digestion under salivary, simulated gastric and small intestinal conditions and fermentation by human gut microbiota. *International Journal of Food Science & Technology, 54*(6), 2277–2287.

Szilagyi, A., Malolepszy, P., Hamard, E., Xue, X., Hilzenrat, N., Ponniah, M., & Chong, G. (2007). Comparison of a real-time polymerase chain reaction assay for lactase genetic polymorphism with standard indirect tests for lactose maldigestion. *Clinical Gastroenterology and Hepatology, 5*(2), 192–196.

Tan, J., McKenzie, C., Potamitis, M., Thorburn, A. N., Mackay, C. R., & Macia, L. (2014). The role of short-chain fatty acids in health and disease. *Advances in Immunology, 121*, 91–119.

Tsai, C. C., Yang, F. L., Huang, Z. Y., Chen, C. S., Yang, Y. L., Hua, K. F., & Wu, S. H. (2012). Oligosaccharide and peptidoglycan of Ganoderma lucidum activate the immune response in human mononuclear cells. *Journal of Agricultural and Food Chemistry, 60*(11), 2830–2837.

van der Hee, B., & Wells, J. M. (2021). Microbial Regulation of Host Physiology by Short-chain Fatty Acids. *Trends in Microbiology, 29*(8), 700–712.

Wang, M., Wichienchot, S., He, X., Fu, X., Huang, Q., & Zhang, B. (2019). In vitro colonic fermentation of dietary fibers: Fermentation rate, short-chain fatty acid production and changes in microbiota. *Trends in Food Science & Technology, 88*, 1–9.

Wang, X., Zhang, M., Zhang, D., Wang, X., Cao, H., Zhang, Q., & Yan, C. (2019). Structural elucidation and anti-osteoporosis activities of polysaccharides obtained from Curculigo orchioides. *Carbohydrate Polymers, 203*, 292–301.

Weir, T. L., Trikha, S. R. J., & Thompson, H. J. (2021). Diet and cancer risk reduction: The role of diet-microbiota interactions and microbial metabolites. *Seminars in Cancer Biology, 70*, 53–60.

Wu, J., Ming, Q., Zhai, X., Wang, S., Zhu, B., Zhang, Q., & Qin, L. (2019). Structure of a polysaccharide from Trichoderma atroviride and its promotion on tanshinones production in Salvia miltiorrhiza hairy roots. *Carbohydrate Polymers, 223*, Article 115125.

Wu, D. T., Yuan, Q., Guo, H., Fu, Y., Li, F., Wang, S. P., & Gan, R. Y. (2021). Dynamic changes of structural characteristics of snow chrysanthemum polysaccharides during in vitro digestion and fecal fermentation and related impacts on gut microbiota. *Food Research International, 141*, Article 109888.

Wu, Y. T., Huo, Y. F., Xu, L., Xu, Y. Y., Wang, X. L., & Zhou, T. (2020). Purification, characterization and antioxidant activity of polysaccharides from Porphyra haitanensis. *International Journal of Biological Macromolecules, 165*(Pt B), 2116–2125.

Yan, J., Shi, S., Wang, H., Liu, R., Li, N., Chen, Y., & Wang, S. (2016). Neutral monosaccharide composition analysis of plant-derived oligo- and polysaccharides by high performance liquid chromatography. *Carbohydrate Polymers, 136*, 1273–1280.

Yang, J., Martinez, I., Walter, J., Keshavarzian, A., & Rose, D. J. (2013). In vitro characterization of the impact of selected dietary fibers on fecal microbiota composition and short chain fatty acid production. *Anaerobe, 23*, 74–81.

Yao, C. K., Muir, J. G., & Gibson, P. R. (2016). Review article: Insights into colonic protein fermentation, its modulation and potential health implications. *Alimentary Pharmacology and Therapeutics, 43*(2), 181–196.

Yu, Q., Jobin, C., & Thomas, R. M. (2021). Implications of the microbiome in the development and treatment of pancreatic cancer: Thinking outside of the box by looking inside the gut. *Neoplasia, 23*(2), 246–256.

Zeng, F., Chen, W., He, P., Zhan, Q., Wang, Q., Wu, H., & Zhang, M. (2020). Structural characterization of polysaccharides with potential antioxidant and immunomodulatory activities from Chinese water chestnut peels. *Carbohydrate Polymers, 246*, Article 116551.

Zhang, Z., Guo, L., Yan, A., Feng, L., & Wan, Y. (2020). Fractionation, structure and conformation characterization of polysaccharides from Anoectochilus roxburghii. *Carbohydrate Polymers, 231*, Article 115688.

Zheng, S., Zhang, W., & Liu, S. (2020). Optimization of ultrasonic-assisted extraction of polysaccharides and triterpenoids from the medicinal mushroom Ganoderma lucidum and evaluation of their in vitro antioxidant capacities. *PLoS One, 15*(12), e0244749.

Zhu, B., Ni, F., Xiong, Q., & Yao, Z. (2021). Marine oligosaccharides originated from seaweeds: Source, preparation, structure, physiological activity and applications. *Critical Reviews in Food Science and Nutrition, 61*(1), 60–74.